

Search for  $B^0 \rightarrow \tau^\pm \mathcal{L}^\mp$  ( $\mathcal{L} = e, \mu$ ) with a hadronic tagging method at Belle

H. Atmacan<sup>16</sup>,<sup>7</sup> A. J. Schwartz,<sup>7</sup> K. Kinoshita,<sup>7</sup> I. Adachi,<sup>19,15</sup> K. Adamczyk,<sup>64</sup> H. Aihara,<sup>88</sup> S. Al Said,<sup>81,40</sup> D. M. Asner,<sup>3</sup> V. Aulchenko,<sup>4,67</sup> T. Aushev,<sup>20</sup> R. Ayad,<sup>81</sup> V. Babu,<sup>8</sup> S. Bahinipati,<sup>24</sup> M. Bauer,<sup>37</sup> P. Behera,<sup>27</sup> K. Belous,<sup>31</sup> J. Bennett,<sup>55</sup> F. Bernlochner,<sup>2</sup> M. Bessner,<sup>18</sup> V. Bhardwaj,<sup>23</sup> B. Bhuyan,<sup>25</sup> T. Bilka,<sup>5</sup> J. Biswal,<sup>36</sup> A. Bobrov,<sup>4,67</sup> A. Bozek,<sup>64</sup> M. Bračko,<sup>52,36</sup> P. Branchini,<sup>33</sup> T. E. Browder,<sup>18</sup> A. Budano,<sup>33</sup> M. Campajola,<sup>32,59</sup> L. Cao,<sup>2</sup> D. Červenkov,<sup>5</sup> M.-C. Chang,<sup>10</sup> P. Chang,<sup>63</sup> V. Chekelian,<sup>53</sup> A. Chen,<sup>61</sup> B. G. Cheon,<sup>17</sup> K. Chilikin,<sup>47</sup> H. E. Cho,<sup>17</sup> K. Cho,<sup>42</sup> S.-K. Choi,<sup>16</sup> Y. Choi,<sup>79</sup> S. Choudhury,<sup>26</sup> D. Cinabro,<sup>92</sup> S. Cunliffe,<sup>8</sup> S. Das,<sup>51</sup> N. Dash,<sup>27</sup> G. De Nardo,<sup>32,59</sup> G. De Pietro,<sup>33</sup> R. Dhamija,<sup>26</sup> F. Di Capua,<sup>32,59</sup> J. Dingfelder,<sup>2</sup> Z. Doležal,<sup>5</sup> T. V. Dong,<sup>11</sup> S. Dubey,<sup>18</sup> D. Epifanov,<sup>4,67</sup> T. Ferber,<sup>8</sup> D. Ferlewicz,<sup>54</sup> A. Frey,<sup>14</sup> B. G. Fulsom,<sup>69</sup> R. Garg,<sup>70</sup> V. Gaur,<sup>91</sup> N. Gabyshev,<sup>4,67</sup> A. Garmash,<sup>4,67</sup> A. Giri,<sup>26</sup> P. Goldenzweig,<sup>37</sup> E. Graziani,<sup>33</sup> D. Greenwald,<sup>83</sup> T. Gu,<sup>72</sup> Y. Guan,<sup>7</sup> K. Gudkova,<sup>4,67</sup> C. Hadjivasiliou,<sup>69</sup> S. Halder,<sup>82</sup> T. Hara,<sup>19,15</sup> O. Hartbrich,<sup>18</sup> K. Hayasaka,<sup>66</sup> H. Hashii,<sup>60</sup> W.-S. Hou,<sup>63</sup> C.-L. Hsu,<sup>80</sup> K. Inami,<sup>58</sup> G. Inguglia,<sup>30</sup> A. Ishikawa,<sup>19,15</sup> R. Itoh,<sup>19,15</sup> M. Iwasaki,<sup>68</sup> Y. Iwasaki,<sup>19</sup> W. W. Jacobs,<sup>28</sup> S. Jia,<sup>11</sup> Y. Jin,<sup>88</sup> K. K. Joo,<sup>6</sup> A. B. Kaliyar,<sup>82</sup> K. H. Kang,<sup>45</sup> Y. Kato,<sup>58</sup> T. Kawasaki,<sup>41</sup> C. Kiesling,<sup>53</sup> C. H. Kim,<sup>17</sup> D. Y. Kim,<sup>77</sup> K.-H. Kim,<sup>94</sup> S. H. Kim,<sup>76</sup> Y.-K. Kim,<sup>94</sup> P. Kodyš,<sup>5</sup> T. Konno,<sup>41</sup> A. Korobov,<sup>4,67</sup> S. Korpar,<sup>52,36</sup> E. Kovalenko,<sup>4,67</sup> P. Križan,<sup>48,36</sup> R. Kroeger,<sup>55</sup> P. Krokovny,<sup>4,67</sup> T. Kuhr,<sup>49</sup> R. Kulasiri,<sup>39</sup> K. Kumara,<sup>92</sup> Y.-J. Kwon,<sup>94</sup> Y.-T. Lai,<sup>38</sup> J. S. Lange,<sup>12</sup> M. Laurenza,<sup>33,74</sup> S. C. Lee,<sup>45</sup> J. Li,<sup>45</sup> L. K. Li,<sup>7</sup> Y. B. Li,<sup>71</sup> L. Li Gioi,<sup>53</sup> J. Libby,<sup>27</sup> K. Lieret,<sup>49</sup> D. Liventsev,<sup>92,19</sup> C. MacQueen,<sup>54</sup> M. Masuda,<sup>87,73</sup> T. Matsuda,<sup>56</sup> D. Matvienko,<sup>4,67,47</sup> M. Merola,<sup>32,59</sup> F. Metzner,<sup>37</sup> K. Miyabayashi,<sup>60</sup> R. Mizuk,<sup>47,20</sup> G. B. Mohanty,<sup>82</sup> R. Mussa,<sup>34</sup> M. Nakao,<sup>19,15</sup> Z. Natkaniec,<sup>64</sup> A. Natochii,<sup>18</sup> L. Nayak,<sup>26</sup> M. Nayak,<sup>84</sup> M. Niiyama,<sup>44</sup> N. K. Nisar,<sup>3</sup> S. Nishida,<sup>19,15</sup> S. Ogawa,<sup>85</sup> H. Ono,<sup>65,66</sup> Y. Onuki,<sup>88</sup> P. Oskin,<sup>47</sup> P. Pakhlov,<sup>47,57</sup> G. Pakhlova,<sup>20,47</sup> S. Pardi,<sup>32</sup> H. Park,<sup>45</sup> S.-H. Park,<sup>19</sup> A. Passeri,<sup>33</sup> S. Paul,<sup>83,53</sup> T. K. Pedlar,<sup>50</sup> R. Pestotnik,<sup>36</sup> L. E. Pilonen,<sup>91</sup> T. Podobnik,<sup>48,36</sup> E. Prencipe,<sup>21</sup> M. T. Prim,<sup>2</sup> I. Ripp-Baudot,<sup>78</sup> A. Rostomyan,<sup>8</sup> N. Rout,<sup>27</sup> G. Russo,<sup>59</sup> D. Sahoo,<sup>82</sup> S. Sandilya,<sup>26</sup> A. Sangal,<sup>7</sup> L. Santelj,<sup>48,36</sup> T. Sanuki,<sup>86</sup> V. Savinov,<sup>72</sup> G. Schnell,<sup>1,22</sup> J. Schueler,<sup>18</sup> C. Schwanda,<sup>30</sup> Y. Seino,<sup>66</sup> K. Senyo,<sup>93</sup> M. E. Sevier,<sup>54</sup> M. Shapkin,<sup>31</sup> C. Sharma,<sup>51</sup> C. P. Shen,<sup>11</sup> J.-G. Shiu,<sup>63</sup> F. Simon,<sup>53</sup> A. Sokolov,<sup>31</sup> E. Solovieva,<sup>47</sup> M. Starič,<sup>36</sup> Z. S. Stottler,<sup>91</sup> M. Sumihama,<sup>13</sup> K. Sumisawa,<sup>19,15</sup> T. Sumiyoshi,<sup>90</sup> W. Sutcliffe,<sup>2</sup> U. Tamponi,<sup>34</sup> K. Tanida,<sup>35</sup> Y. Tao,<sup>9</sup> F. Tenchini,<sup>8</sup> K. Trabelsi,<sup>46</sup> M. Uchida,<sup>89</sup> T. Uglov,<sup>47,20</sup> Y. Unno,<sup>17</sup> K. Uno,<sup>66</sup> S. Uno,<sup>19,15</sup> P. Urquijo,<sup>54</sup> S. E. Vahsen,<sup>18</sup> R. Van Tonder,<sup>2</sup> G. Varner,<sup>18</sup> K. E. Varvell,<sup>80</sup> A. Vinokurova,<sup>4,67</sup> E. Waheed,<sup>19</sup> C. H. Wang,<sup>62</sup> E. Wang,<sup>72</sup> M.-Z. Wang,<sup>63</sup> P. Wang,<sup>29</sup> X. L. Wang,<sup>11</sup> M. Watanabe,<sup>66</sup> S. Watanuki,<sup>46</sup> J. Wiechczynski,<sup>64</sup> E. Won,<sup>43</sup> B. D. Yabsley,<sup>80</sup> W. Yan,<sup>75</sup> S. B. Yang,<sup>43</sup> H. Ye,<sup>8</sup> J. Yelton,<sup>9</sup> J. H. Yin,<sup>43</sup> Z. P. Zhang,<sup>75</sup> V. Zhilich,<sup>4,67</sup> and V. Zhukova<sup>47</sup>

(The Belle Collaboration)

<sup>1</sup>Department of Physics, University of the Basque Country UPV/EHU, 48080 Bilbao<sup>2</sup>University of Bonn, 53115 Bonn<sup>3</sup>Brookhaven National Laboratory, Upton, New York 11973<sup>4</sup>Budker Institute of Nuclear Physics SB RAS, Novosibirsk 630090<sup>5</sup>Faculty of Mathematics and Physics, Charles University, 121 16 Prague<sup>6</sup>Chonnam National University, Gwangju 61186<sup>7</sup>University of Cincinnati, Cincinnati, Ohio 45221<sup>8</sup>Deutsches Elektronen-Synchrotron, 22607 Hamburg<sup>9</sup>University of Florida, Gainesville, Florida 32611<sup>10</sup>Department of Physics, Fu Jen Catholic University, Taipei 24205<sup>11</sup>Key Laboratory of Nuclear Physics and Ion-beam Application (MOE) and Institute of Modern Physics, Fudan University, Shanghai 200443<sup>12</sup>Justus-Liebig-Universität Gießen, 35392 Gießen<sup>13</sup>Gifu University, Gifu 501-1193<sup>14</sup>II. Physikalisches Institut, Georg-August-Universität Göttingen, 37073 Göttingen<sup>15</sup>SOKENDAI (The Graduate University for Advanced Studies), Hayama 240-0193<sup>16</sup>Gyeongsang National University, Jinju 52828<sup>17</sup>Department of Physics and Institute of Natural Sciences, Hanyang University, Seoul 04763<sup>18</sup>University of Hawaii, Honolulu, Hawaii 96822<sup>19</sup>High Energy Accelerator Research Organization (KEK), Tsukuba 305-0801<sup>20</sup>National Research University Higher School of Economics, Moscow 101000<sup>21</sup>Forschungszentrum Jülich, 52425 Jülich<sup>22</sup>IKERBASQUE, Basque Foundation for Science, 48013 Bilbao<sup>23</sup>Indian Institute of Science Education and Research Mohali, SAS Nagar 140306

- <sup>24</sup>Indian Institute of Technology Bhubaneswar, Satya Nagar 751007
- <sup>25</sup>Indian Institute of Technology Guwahati, Assam 781039
- <sup>26</sup>Indian Institute of Technology Hyderabad, Telangana 502285
- <sup>27</sup>Indian Institute of Technology Madras, Chennai 600036
- <sup>28</sup>Indiana University, Bloomington, Indiana 47408
- <sup>29</sup>Institute of High Energy Physics, Chinese Academy of Sciences, Beijing 100049
- <sup>30</sup>Institute of High Energy Physics, Vienna 1050
- <sup>31</sup>Institute for High Energy Physics, Protvino 142281
- <sup>32</sup>INFN—Sezione di Napoli, I-80126 Napoli
- <sup>33</sup>INFN—Sezione di Roma Tre, I-00146 Rome
- <sup>34</sup>INFN—Sezione di Torino, I-10125 Torino
- <sup>35</sup>Advanced Science Research Center, Japan Atomic Energy Agency, Naka 319-1195
- <sup>36</sup>J. Stefan Institute, 1000 Ljubljana
- <sup>37</sup>Institut für Experimentelle Teilchenphysik, Karlsruher Institut für Technologie, 76131 Karlsruhe
- <sup>38</sup>Kavli Institute for the Physics and Mathematics of the Universe (WPI),  
University of Tokyo, Kashiwa 277-8583
- <sup>39</sup>Kennesaw State University, Kennesaw, Georgia 30144
- <sup>40</sup>Department of Physics, Faculty of Science, King Abdulaziz University, Jeddah 21589
- <sup>41</sup>Kitasato University, Sagami-hara 252-0373
- <sup>42</sup>Korea Institute of Science and Technology Information, Daejeon 34141
- <sup>43</sup>Korea University, Seoul 02841
- <sup>44</sup>Kyoto Sangyo University, Kyoto 603-8555
- <sup>45</sup>Kyungpook National University, Daegu 41566
- <sup>46</sup>Université Paris-Saclay, CNRS/IN2P3, IJCLab, 91405 Orsay
- <sup>47</sup>P.N. Lebedev Physical Institute of the Russian Academy of Sciences, Moscow 119991
- <sup>48</sup>Faculty of Mathematics and Physics, University of Ljubljana, 1000 Ljubljana
- <sup>49</sup>Ludwig Maximilians University, 80539 Munich
- <sup>50</sup>Luther College, Decorah, Iowa 52101
- <sup>51</sup>Malaviya National Institute of Technology Jaipur, Jaipur 302017
- <sup>52</sup>Faculty of Chemistry and Chemical Engineering, University of Maribor, 2000 Maribor
- <sup>53</sup>Max-Planck-Institut für Physik, 80805 München
- <sup>54</sup>School of Physics, University of Melbourne, Victoria 3010
- <sup>55</sup>University of Mississippi, University, Mississippi 38677
- <sup>56</sup>University of Miyazaki, Miyazaki 889-2192
- <sup>57</sup>Moscow Physical Engineering Institute, Moscow 115409
- <sup>58</sup>Graduate School of Science, Nagoya University, Nagoya 464-8602
- <sup>59</sup>Università di Napoli Federico II, I-80126 Napoli
- <sup>60</sup>Nara Women's University, Nara 630-8506
- <sup>61</sup>National Central University, Chung-li 32054
- <sup>62</sup>National United University, Miao Li 36003
- <sup>63</sup>Department of Physics, National Taiwan University, Taipei 10617
- <sup>64</sup>H. Niewodniczanski Institute of Nuclear Physics, Krakow 31-342
- <sup>65</sup>Nippon Dental University, Niigata 951-8580
- <sup>66</sup>Niigata University, Niigata 950-2181
- <sup>67</sup>Novosibirsk State University, Novosibirsk 630090
- <sup>68</sup>Osaka City University, Osaka 558-8585
- <sup>69</sup>Pacific Northwest National Laboratory, Richland, Washington 99352
- <sup>70</sup>Panjab University, Chandigarh 160014
- <sup>71</sup>Peking University, Beijing 100871
- <sup>72</sup>University of Pittsburgh, Pittsburgh, Pennsylvania 15260
- <sup>73</sup>Research Center for Nuclear Physics, Osaka University, Osaka 567-0047
- <sup>74</sup>Dipartimento di Matematica e Fisica, Università di Roma Tre, I-00146 Rome
- <sup>75</sup>Department of Modern Physics and State Key Laboratory of Particle Detection and Electronics,  
University of Science and Technology of China, Hefei 230026
- <sup>76</sup>Seoul National University, Seoul 08826
- <sup>77</sup>Soongsil University, Seoul 06978
- <sup>78</sup>Université de Strasbourg, CNRS, IPHC, UMR 7178, 67037 Strasbourg
- <sup>79</sup>Sungkyunkwan University, Suwon 16419
- <sup>80</sup>School of Physics, University of Sydney, New South Wales 2006
- <sup>81</sup>Department of Physics, Faculty of Science, University of Tabuk, Tabuk 71451

<sup>82</sup>Tata Institute of Fundamental Research, Mumbai 400005<sup>83</sup>Department of Physics, Technische Universität München, 85748 Garching<sup>84</sup>School of Physics and Astronomy, Tel Aviv University, Tel Aviv 69978<sup>85</sup>Toho University, Funabashi 274-8510<sup>86</sup>Department of Physics, Tohoku University, Sendai 980-8578<sup>87</sup>Earthquake Research Institute, University of Tokyo, Tokyo 113-0032<sup>88</sup>Department of Physics, University of Tokyo, Tokyo 113-0033<sup>89</sup>Tokyo Institute of Technology, Tokyo 152-8550<sup>90</sup>Tokyo Metropolitan University, Tokyo 192-0397<sup>91</sup>Virginia Polytechnic Institute and State University, Blacksburg, Virginia 24061<sup>92</sup>Wayne State University, Detroit, Michigan 48202<sup>93</sup>Yamagata University, Yamagata 990-8560<sup>94</sup>Yonsei University, Seoul 03722

(Received 22 August 2021; accepted 18 October 2021; published 29 November 2021)

We present a search for the lepton-flavor-violating decays  $B^0 \rightarrow \tau^\pm \ell^\mp$ , where  $\ell = (e, \mu)$ , using the full data sample of  $772 \times 10^6$   $B\bar{B}$  pairs recorded by the Belle detector at the KEKB asymmetric-energy  $e^+e^-$  collider. We use events in which one  $B$  meson is fully reconstructed in a hadronic decay mode. The  $\tau^\pm$  lepton is reconstructed indirectly using the momentum of the reconstructed  $B$  and that of the  $\ell^\mp$  from the signal decay. We find no evidence for  $B^0 \rightarrow \tau^\pm \ell^\mp$  decays and set upper limits on their branching fractions at 90% confidence level of  $\mathcal{B}(B^0 \rightarrow \tau^\pm \mu^\mp) < 1.5 \times 10^{-5}$  and  $\mathcal{B}(B^0 \rightarrow \tau^\pm e^\mp) < 1.6 \times 10^{-5}$ .

DOI: 10.1103/PhysRevD.104.L091105

## I. INTRODUCTION

The lepton-flavor-violating decays  $B^0 \rightarrow \tau^\pm \ell^\mp$  [1], where  $\ell = (e, \mu)$ , are promising modes in which to search for new physics. Recently, there have been indications of possible violation of lepton flavor universality (LFU) in  $B^0 \rightarrow D^{(*)-} \tau^+ \nu$  [2],  $B^0 \rightarrow K^{*0} \ell^+ \ell^-$  [3], and  $B^\pm \rightarrow K^\pm \ell^+ \ell^-$  [4,5] decays. Other studies are less conclusive [6,7]. LFU violation is often accompanied by lepton flavor violation (LFV) in theoretical models [8]. The decay  $B^0 \rightarrow \tau^\pm \ell^\mp$ , like  $B^0 \rightarrow D^{(*)-} \tau^+ \nu$ , connects a third-generation quark with a third-generation lepton. The decay can occur in principle via neutrino mixing [9]; however, the rate due to such mixing [10] is considerably below current or future experimental sensitivities. Thus, observing these decays would indicate new physics. Some new physics models give rise to branching fractions of  $10^{-9}$  to  $10^{-10}$ . For example, Pati-Salam vector leptoquarks of mass  $86 \text{ TeV}/c^2$  give branching fractions of  $4.4 \times 10^{-9}$  for  $B^0 \rightarrow \tau^\pm \mu^\mp$  and  $1.6 \times 10^{-9}$  for  $B^0 \rightarrow \tau^\pm e^\mp$  [11]. The general flavor-universal minimal supersymmetric Standard Model predicts branching fractions of up to about  $2 \times 10^{-10}$  [12].

These decay modes have previously been studied by the CLEO [13], BABAR [14], and LHCb [15] experiments.

No evidence for these decays has been found. The current most stringent upper limits are  $\mathcal{B}(B^0 \rightarrow \tau^\pm \mu^\mp) < 1.2 \times 10^{-5}$  [15] and  $\mathcal{B}(B^0 \rightarrow \tau^\pm e^\mp) < 2.8 \times 10^{-5}$  [14], both at 90% confidence level (CL). In this paper we report a search for  $B^0 \rightarrow \tau^\pm \ell^\mp$  decays using the full Belle data sample of  $711 \text{ fb}^{-1}$  recorded at the  $\Upsilon(4S)$  resonance. This is the first such search from Belle.

## II. DATASET AND DETECTOR DESCRIPTION

Our data sample consists of  $(772 \pm 11) \times 10^6$   $B\bar{B}$  pairs produced in  $e^+e^- \rightarrow \Upsilon(4S)$  events recorded by the Belle detector at the KEKB asymmetric-energy  $e^+e^-$  collider [16]. The Belle detector is a large-solid-angle magnetic spectrometer that consists of a silicon vertex detector (SVD), a 50-layer central drift chamber (CDC), an array of aerogel threshold Cherenkov counters (ACC), a barrel-like arrangement of time-of-flight (TOF) scintillation counters, and an electromagnetic calorimeter comprising CsI(Tl) crystals (ECL). All these detectors are located inside a superconducting solenoid coil that provides a 1.5 T magnetic field. An iron flux return yoke located outside the coil is instrumented with resistive-plate chambers (KLM) to detect  $K_L^0$  mesons and to identify muons. Two inner detector configurations were used: for the first  $152 \times 10^6$   $B\bar{B}$  pairs, a 2.0 cm radius beam pipe and a three-layer SVD were used; and for the remaining  $620 \times 10^6$   $B\bar{B}$  pairs, a 1.5 cm radius beam pipe, a four-layer SVD [17], and a small-cell inner drift chamber were used. A more detailed description of the detector is provided in Ref. [18].

Published by the American Physical Society under the terms of the Creative Commons Attribution 4.0 International license. Further distribution of this work must maintain attribution to the author(s) and the published article's title, journal citation, and DOI. Funded by SCOAP<sup>3</sup>.

We study properties of signal events, sources of background, and optimize selection criteria using Monte Carlo (MC) simulated events. These samples are generated using the software packages EVTGEN [19] and PYTHIA [20], and final-state radiation is included via PHOTOS [21]. The detector response is simulated using GEANT3 [22]. We produce  $B^0 \rightarrow \tau^\pm \ell^\mp$  MC events to calculate signal reconstruction efficiencies. To estimate backgrounds, we use MC samples that describe all  $e^+e^- \rightarrow q\bar{q}$  processes. Events containing  $e^+e^- \rightarrow B\bar{B}$  with subsequent  $b \rightarrow cW$  decay, and  $e^+e^- \rightarrow q\bar{q}$  ( $q = u, d, s, c$ ) continuum events, are both simulated with five times the integrated luminosity of Belle. Semileptonic  $b \rightarrow u\ell\nu$  decays are simulated with 20 times the integrated luminosity. Rare  $b \rightarrow s$  and  $b \rightarrow u$  decays are simulated with 50 times the integrated luminosity.

### III. EVENT SELECTION

Our analysis uses a technique uniquely suited to  $e^+e^-$  flavor factory experiments, in which the energy and momentum of the initial state are known. We first reconstruct a  $B$  meson decaying hadronically; this is referred to as the ‘‘tag-side’’  $B$  meson ( $B_{\text{tag}}$ ). We use the reconstructed  $B_{\text{tag}}$  momentum and the  $e^+e^-$  initial momentum to infer the momentum of the signal-side  $B$  meson ( $B_{\text{sig}}$ ). Because  $B^0 \rightarrow \tau^\pm \ell^\mp$  are two-body decays, the momentum of the  $\tau$  lepton can be inferred from the momentum of  $B_{\text{sig}}$  and the momentum of  $\ell^\mp$ ; thus, the  $\tau^\pm$  does not need to be reconstructed. We define the ‘‘missing mass’’ as

$$M_{\text{miss}} = \sqrt{(E_{B_{\text{sig}}} - E_\ell)^2/c^4 - (\vec{p}_{B_{\text{sig}}} - \vec{p}_\ell)^2/c^2}, \quad (1)$$

where  $E_{B_{\text{sig}}}$  and  $\vec{p}_{B_{\text{sig}}}$  are the energy and momentum, respectively, of  $B_{\text{sig}}$ , and  $E_\ell$  and  $\vec{p}_\ell$  are the corresponding quantities for  $\ell^\mp$ . The quantity  $M_{\text{miss}}$  is the invariant mass of the unreconstructed or missing particle and, for  $B^0 \rightarrow \tau^\pm \ell^\mp$  decays, should peak at the mass of the  $\tau$  lepton ( $m_\tau = 1.776 \text{ GeV}/c^2$  [23]). To improve the resolution in  $M_{\text{miss}}$ , we evaluate it in the  $e^+e^-$  center-of-mass (c.m.) frame and substitute the beam energy  $E_{\text{beam}}$  for  $E_{B_{\text{sig}}}$ . To avoid introducing bias in our analysis, we analyze the data in a ‘‘blind’’ manner, i.e., we finalize all selection criteria before viewing events in a region around  $m_\tau$ . This blinded region is  $[1.65, 1.90] \text{ GeV}/c^2$ , which corresponds to approximately  $3.8\sigma$  in the resolution.

#### A. Tag-side selection

We first reconstruct  $B_{\text{tag}}$  candidates in one of 1104 hadronic decay channels using a hierarchical algorithm based on the NeuroBayes neural network package [24]. The quality of  $B_{\text{tag}}$  is represented by a single classifier output,  $O_{\text{NN}}$ , which ranges from 0 (backgroundlike) to 1 (signal-like). The output  $O_{\text{NN}}$  is mainly determined by the

$B_{\text{tag}}$  reconstruction. It includes event-shape information and significantly suppresses  $e^+e^- \rightarrow q\bar{q}$  continuum events. In addition to  $O_{\text{NN}}$ , two other variables are used for selecting  $B_{\text{tag}}$  candidates: the energy difference  $\Delta E \equiv E_{B_{\text{tag}}} - E_{\text{beam}}$ , and the beam-energy-constrained mass  $M_{\text{bc}} \equiv \sqrt{E_{\text{beam}}^2/c^4 - |\vec{p}_{B_{\text{tag}}}|^2/c^2}$ , where  $E_{B_{\text{tag}}}$  and  $\vec{p}_{B_{\text{tag}}}$  are the reconstructed energy and momentum, respectively, of  $B_{\text{tag}}$ . These quantities are evaluated in the  $e^+e^-$  c.m. system. The  $B_{\text{tag}}$  candidate is required to satisfy  $|\Delta E| < 0.05 \text{ GeV}$ . For each signal mode, we choose selection criteria on  $O_{\text{NN}}$  and  $M_{\text{bc}}$  by optimizing a figure of merit (FOM). The FOM is defined as  $\varepsilon_{\text{MC}}/\sqrt{N_{\text{B}}}$ , where  $\varepsilon_{\text{MC}}$  is the reconstruction efficiency of signal events as determined from MC simulation, and  $N_{\text{B}}$  is the number of background events expected within the signal region  $M_{\text{miss}} \in [1.65, 1.90] \text{ GeV}/c^2$ . Based on FOM studies, we require  $O_{\text{NN}} > 0.082$  for  $B^0 \rightarrow \tau^\pm \mu^\mp$ ,  $O_{\text{NN}} > 0.095$  for  $B^0 \rightarrow \tau^\pm e^\mp$ , and  $M_{\text{bc}} > 5.272 \text{ GeV}/c^2$  for both modes.

After all  $B_{\text{tag}}$  selection criteria are applied, about 10% of  $B^0 \rightarrow \tau^\pm \mu^\mp$  events and 8% of  $B^0 \rightarrow \tau^\pm e^\mp$  events have multiple  $B_{\text{tag}}$  candidates. For such events, we select a single  $B_{\text{tag}}$  by choosing the candidate with the highest value of  $O_{\text{NN}}$ . This criterion selects the correct candidate 90% of the time, according to MC simulation.

#### B. Signal-side selection

To reconstruct the signal side, only tracks not associated with  $B_{\text{tag}}$  are considered. Such tracks are required to originate from the interaction point (IP) and have an impact parameter  $|dz| < 4.0 \text{ cm}$  along the  $z$  axis, which points opposite the  $e^+$  beam direction. We also require  $dr < 2.0 \text{ cm}$  in the  $x$ - $y$  plane (transverse to the  $e^+$  beam direction), where  $dr = \sqrt{dx^2 + dy^2}$ .

Charged tracks are identified by combining information from various subdetectors into a likelihood function  $\mathcal{L}_i$ , where  $i = e, \mu, \pi, K, \text{ or } p$  [25]. Muon candidates are identified based on the response of the CDC and KLM [26]. A track with a likelihood ratio  $\mathcal{R}_\mu = \mathcal{L}_\mu/(\mathcal{L}_\mu + \mathcal{L}_\pi + \mathcal{L}_K) > 0.90$  is identified as a muon. The detection efficiency of this requirement is about 89%, and the pion misidentification rate is about 2%. Electron candidates are identified mainly using the ratio of the energy deposited in the ECL to the track momentum, the shower shape in the ECL, and the energy loss in the CDC. A track with a likelihood ratio  $\mathcal{R}_e = \mathcal{L}_e/(\mathcal{L}_e + \mathcal{L}_{\text{hadrons}}) > 0.90$  is identified as an electron, where  $\mathcal{L}_{\text{hadrons}}$  is the product of probability density functions (PDFs) for hadrons [27]. The efficiency of this requirement is about 94%, and the pion misidentification rate is about 0.3%. We recover electron energy lost due to bremsstrahlung by searching for photons within a cone of radius 50 mrad centered around the electron momentum. If such a photon is found,

its four-momentum (assuming it originated at the IP) is added to that of the electron.

We require that  $M_{\text{miss}}$  be in the range 1.40 to 2.20  $\text{GeV}/c^2$ . Every muon or electron candidate satisfying this requirement is treated as a  $B_{\text{sig}}$  candidate. After these selections, we find that less than 1% of  $B^0 \rightarrow \tau^\pm \mu^\mp$  and  $B^0 \rightarrow \tau^\pm e^\mp$  events have multiple  $B_{\text{sig}}$  candidates. These fractions are consistent with those from MC simulations. For such events, in order to preserve efficiency, we retain all such candidates, i.e., we do not apply a best-candidate selection.

### C. Background

After applying all selection criteria, a small amount of background remains. This background is studied using MC simulation and found to originate mainly from  $b \rightarrow cW$  and  $b \rightarrow u\ell\nu$  decays. These backgrounds are smoothly falling in the  $M_{\text{miss}}$  distribution. However, for  $B^0 \rightarrow \tau^\pm \mu^\mp$  candidates, two small peaks are observed: one at  $M_{\text{miss}} \approx 1.869 \text{ GeV}/c^2$  and the other at  $M_{\text{miss}} \approx 2.010 \text{ GeV}/c^2$ . The former corresponds to  $B^0 \rightarrow D^-\pi^+$  decays, while the latter corresponds to  $B^0 \rightarrow D^{*-}\pi^+$  decays, where in both cases the  $\pi^+$  is misidentified as  $\mu^+$ . These  $B^0 \rightarrow D^{(*)-}\pi^+$  decays are taken into account when fitting the  $M_{\text{miss}}$  distribution for the signal yield (described below).

### D. Control samples

We use control samples of  $B^0 \rightarrow D^{(*)-}\pi^+$  decays to determine corrections to the shapes of the  $B^0 \rightarrow \tau^\pm \ell^\mp$  PDFs used to fit for the signal yields (see Sec. IV). To identify  $B^0 \rightarrow D^{(*)-}\pi^+$  decays, we select pions on the signal side rather than leptons. Pion candidates are identified using  $dE/dx$  measured in the CDC, time-of-flight information from the TOF, and the photon yield in the ACC. A track with a likelihood ratio  $\mathcal{R}_\pi = \mathcal{L}_\pi / (\mathcal{L}_\pi + \mathcal{L}_K) > 0.90$  is identified as a pion [25]. All other selection criteria are the same as for the  $B^0 \rightarrow \tau^\pm \ell^\mp$  search. In addition, we veto leptons by requiring that  $\mathcal{R}_\mu < 0.90$  and  $\mathcal{R}_e < 0.90$ . With the above selection, the pion identification efficiency is about 95%, and the kaon misidentification rate is about 5%.

## IV. MAXIMUM LIKELIHOOD FITS

We determine the  $B^0 \rightarrow \tau^\pm \ell^\mp$  signal yields by performing an unbinned extended maximum-likelihood fit to the  $M_{\text{miss}}$  distributions. The PDF used to model correctly reconstructed signal decays is a double Gaussian for  $B^0 \rightarrow \tau^\pm \mu^\mp$  and the sum of three Gaussians for  $B^0 \rightarrow \tau^\pm e^\mp$ . These Gaussians are allowed to have different means. We also model misreconstructed signal decays in which the lepton selected is subject to final-state radiation or is not a direct daughter in the two-body  $B^0 \rightarrow \tau^\pm \ell^\mp$  decay, i.e., it originates from  $\tau^\pm \rightarrow \ell^\pm \nu \bar{\nu}$  or  $\tau^\pm \rightarrow \pi^\pm (\rightarrow \ell^\pm \nu) \bar{\nu}$ . This

component is referred to as a ‘‘self-cross-feed’’ signal, and we model it with a double Gaussian and an exponential function. The fractions of self-cross-feed signal are fixed to the values obtained from MC simulation:  $(5.0 \pm 0.2)\%$  for  $B^0 \rightarrow \tau^\pm \mu^\mp$  and  $(14.0 \pm 0.3)\%$  for  $B^0 \rightarrow \tau^\pm e^\mp$ . The self-cross-feed fraction is larger for the electron channel due to a larger contribution from  $B^0 \rightarrow \tau^\pm e^\mp \gamma$  decays.

The shape parameters of the signal PDFs are obtained from MC simulations. We make corrections to these to account for small differences observed between the MC simulation and data. We obtain these correction factors by fitting the  $M_{\text{miss}}$  distributions of the high-statistics  $B^0 \rightarrow D^{(*)-}\pi^+$  control samples. For the  $B^0 \rightarrow D^{(*)-}\pi^+$  samples, we fit both data and MC events and record small shifts observed in the means of the PDFs, and nominal differences in the widths. We apply these shifts for the means and scaling factors for the widths to the  $B^0 \rightarrow \tau^\pm \ell^\mp$  signal PDFs. The uncertainties in these correction factors are accounted for when evaluating systematic uncertainties.

Background PDFs of all modes are modeled with exponential functions. The shape parameters for these background PDFs are all floated, along with the background and signal yields. The PDFs for misidentified  $B^0 \rightarrow D^-\pi^+$  and  $B^0 \rightarrow D^{*-}\pi^+$  decays are taken to be a double Gaussian and the sum of three Gaussians, respectively.

We validate our fitting procedure and check for fit bias using MC simulations. We generate large ensembles of simulated experiments, in which the  $M_{\text{miss}}$  distributions are generated from the PDFs used for fitting. We fit these ensembles and find that the fitted signal yields are consistent with the input values; the mean difference is

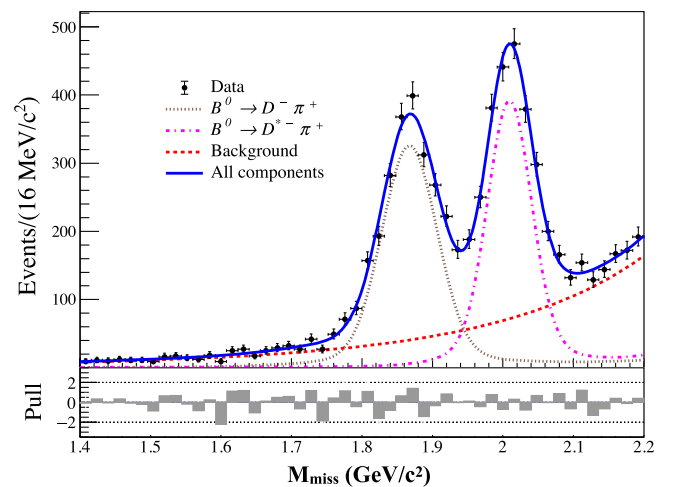


FIG. 1. The  $M_{\text{miss}}$  distribution of  $B^0 \rightarrow D^{(*)-}\pi^+$  candidates observed in data (black dots) along with projections of the fit result: the overall fit result (solid blue curve), the background component (dashed red curve), the  $B^0 \rightarrow D^-\pi^+$  component (dotted brown curve) and the  $B^0 \rightarrow D^{*-}\pi^+$  component (dash-dotted magenta curve). The plot below the distribution shows the residuals divided by the errors (pulls).

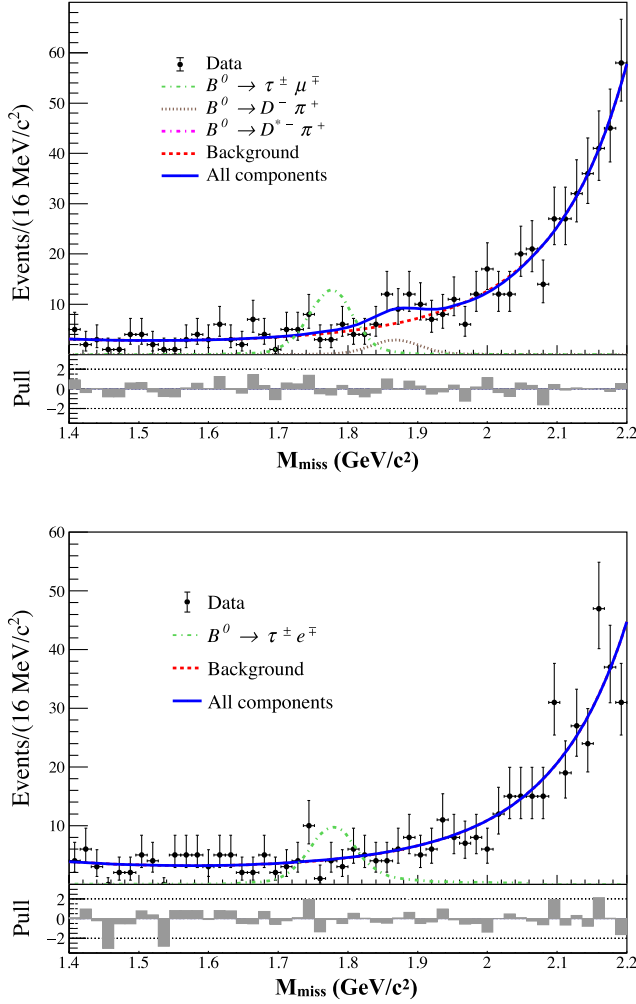


FIG. 2. The  $M_{\text{miss}}$  distributions of  $B^0 \rightarrow \tau^\pm \mu^\mp$  (upper) and  $B^0 \rightarrow \tau^\pm e^\mp$  (lower) candidates, along with projections of the fit result. The black dots show the data, the dashed red curve shows the background component, and the solid blue curve shows the overall fit result. The dash-dotted green curve shows the signal PDF, with a normalization corresponding to a branching fraction of  $10^{-4}$ . In the upper plot, the dotted brown curve shows the  $B^0 \rightarrow D^- \pi^+$  component. The plots below the distributions show the residuals divided by the errors (pulls).

$-0.08 \pm 0.05$  events for  $B^0 \rightarrow \tau^\pm \mu^\mp$  and  $-0.00 \pm 0.05$  events for  $B^0 \rightarrow \tau^\pm e^\mp$ . We include these small potential biases when evaluating systematic uncertainties. We also fit ensembles of fully simulated events and again find the signal yields to be consistent with the input values.

To further check our analysis procedure and acceptance calculation, we measure the branching fractions for the control channels  $B^0 \rightarrow D^{(*)-} \pi^+$ . The  $M_{\text{miss}}$  distributions of these decays along with projections of the fit result are shown in Fig. 1. To assess the goodness of fit, we calculate a  $\chi^2$  statistic from the residuals of the fit result. Dividing by the number of degrees of freedom ( $n_{\text{dof}}$ ) gives  $\chi^2/n_{\text{dof}} = 0.89$ , where  $n_{\text{dof}}$  is 41. The fitted yields are

$2136 \pm 71$  and  $2071 \pm 74$  for  $B^0 \rightarrow D^- \pi^+$  and  $B^0 \rightarrow D^{*-} \pi^+$ , respectively, and the resulting branching fractions are  $\mathcal{B}(B^0 \rightarrow D^- \pi^+) = (2.54 \pm 0.11) \times 10^{-3}$  and  $\mathcal{B}(B^0 \rightarrow D^{*-} \pi^+) = (2.67 \pm 0.12) \times 10^{-3}$ , where the uncertainties listed are statistical only. These values are in excellent agreement with the current world averages  $\mathcal{B}(B^0 \rightarrow D^- \pi^+) = (2.52 \pm 0.13) \times 10^{-3}$  and  $\mathcal{B}(B^0 \rightarrow D^{*-} \pi^+) = (2.74 \pm 0.12) \times 10^{-3}$  [23].

The  $M_{\text{miss}}$  distributions for signal  $B^0 \rightarrow \tau^\pm \ell^\mp$  decays along with projections of the fit result are shown in Fig. 2. The  $\chi^2/n_{\text{dof}}$  values are 0.54 ( $n_{\text{dof}} = 44$ ) and 0.70 ( $n_{\text{dof}} = 44$ ) for  $B^0 \rightarrow \tau^\pm \mu^\mp$  and  $B^0 \rightarrow \tau^\pm e^\mp$ , respectively. The fitted signal yields are  $N_{\text{sig}} = 1.8^{+8.2}_{-7.6}$  for  $B^0 \rightarrow \tau^\pm \mu^\mp$  and  $N_{\text{sig}} = 0.3^{+8.8}_{-8.2}$  for  $B^0 \rightarrow \tau^\pm e^\mp$ . Both yields are consistent with zero. In the  $B^0 \rightarrow \tau^\pm \mu^\mp$  sample, we observe  $(17 \pm 10)$   $B^0 \rightarrow D^- \pi^+$  events and  $(-2 \pm 12)$   $B^0 \rightarrow D^{*-} \pi^+$  events; these yields are consistent with expectations based on MC simulation.

## V. UPPER LIMIT CALCULATION

We calculate upper limits on  $N_{\text{sig}}$  and the branching fractions at 90% CL using a frequentist method. We first generate sets of MC-simulated events, with each set being equivalent to the Belle data sample. Both signal and background events are generated according to their respective PDFs. The number of background events generated is equal to that obtained from the data fit. We vary the number of input signal events, and for each value we generate an ensemble of 10 000 data sets. We fit these data sets and calculate the fraction ( $f_{\text{sig}}$ ) that has a fitted signal yield less than that obtained from the Belle data (1.8 or 0.3 events). Our 90% CL upper limit on the number of signal events ( $N_{\text{sig}}^{\text{UL}}$ ) is the number of input signal events that has  $f_{\text{sig}} = 0.10$ . We convert  $N_{\text{sig}}^{\text{UL}}$  to an upper limit on the branching fraction ( $\mathcal{B}^{\text{UL}}$ ) via the formula

$$\mathcal{B}^{\text{UL}} = \frac{N_{\text{sig}}^{\text{UL}}}{2 \times N_{B\bar{B}} \times f^{00} \times \varepsilon}. \quad (2)$$

In this expression,  $N_{B\bar{B}}$  is the number of  $B\bar{B}$  pairs;  $f^{00} = 0.486 \pm 0.006$  is the fraction that are  $B^0 \bar{B}^0$  [23]; and  $\varepsilon$  is the signal efficiency including tag-side branching fractions and reconstruction efficiencies.

We include systematic uncertainties (discussed below) in  $\mathcal{B}^{\text{UL}}$  as follows. We divide all systematic uncertainties into two types (see Table II): those arising from the numerator of Eq. (2) (“additive” uncertainties), and those arising from the denominator of Eq. (2) (“multiplicative” uncertainties). Additive uncertainties arise from fitting for the signal yield, while multiplicative uncertainties correspond to the number of  $B$  decays reconstructed. We account for the latter when generating MC data sets in our frequentist procedure. The number of signal events is varied randomly around the

TABLE I. Summary of the fit results for  $N_{\text{sig}}$ , and the resulting 90% CL upper limits  $N_{\text{sig}}^{\text{UL}}$  and  $\mathcal{B}^{\text{UL}}$  (see text).

Mode	$\epsilon$ ( $\times 10^{-4}$ )	$N_{\text{sig}}$	$N_{\text{sig}}^{\text{UL}}$	$\mathcal{B}^{\text{UL}}$ ( $\times 10^{-5}$ )
$B^0 \rightarrow \tau^\pm \mu^\mp$	11.0	$1.8^{+8.2}_{-7.6}$	12.4	1.5
$B^0 \rightarrow \tau^\pm e^\mp$	9.8	$0.3^{+8.8}_{-8.2}$	11.6	1.6

nominal input value by the total multiplicative uncertainty. Subsequently, after fitting an MC data set, we adjust the fitted value  $N_{\text{sig}}$  by a value sampled from a Gaussian distribution with mean zero and a width equal to the total additive uncertainty. As a final step, to include possible fit bias, this value is shifted by an amount obtained by sampling a Gaussian distribution with a mean equal to the fit bias discussed earlier (the central value) and a width equal to the uncertainty in the bias. This final value is used when calculating  $f_{\text{sig}}$ . The resulting upper limits for  $N_{\text{sig}}^{\text{UL}}$  and  $\mathcal{B}^{\text{UL}}$  are listed in Table I. These values are the same as the upper limits expected based on MC ( $1.6 \times 10^{-5}$  for both modes), reflecting good agreement between the background levels observed in data and the MC.

## VI. SYSTEMATIC UNCERTAINTIES

The systematic uncertainties in our measurement—aside from potential fit bias, which is treated separately when setting the upper limits—are listed in Table II. Uncertainties in the shapes of the PDFs used for the signal are evaluated by varying all fixed parameters by  $\pm 1\sigma$ ; the resulting change in the signal yield is taken as the systematic uncertainty. The fixed parameters that are varied include the correction factors to the shapes as obtained from the  $B^0 \rightarrow D^{(*)-} \pi^+$  control samples. The fraction of

TABLE II. Systematic uncertainties for the branching fraction measurement. Those listed in the upper section (“additive”) arise from fitting for the signal yield and are listed in number of events; those in the lower section (“multiplicative”) arise from the number of reconstructed  $B$  decays and are listed in percent.

Source	$B^0 \rightarrow \tau^\pm \mu^\mp$	$B^0 \rightarrow \tau^\pm e^\mp$
PDF shapes	0.7	0.3
Self-cross-feed fraction	< 0.1	0.1
Total (events)	0.7	0.3
$B_{\text{tag}}$	4.5	4.5
Track reconstruction	0.3	0.3
Lepton identification	1.6	1.8
MC statistics	< 0.1	< 0.1
Number of $B\bar{B}$ pairs	1.4	1.4
$f^{00}$ ( $B\bar{B} \rightarrow B^0 \bar{B}^0$ fraction)	1.2	1.2
Total (%)	5.1	5.2

the self-cross-feed signal is fixed to the MC value. We vary this fraction by  $\pm 50\%$  and take the resulting change in the signal yield as the systematic uncertainty.

The reconstruction efficiency for  $B_{\text{tag}}$  is evaluated via MC simulation. However, there is uncertainty arising from branching fractions for tagging modes that are not well measured, and from unknown decay dynamics of multi-body hadronic decays. To account for these effects, a correction factor to the reconstruction efficiency is applied. This correction is evaluated as done in Ref. [28], by comparing the number of events containing both a  $B_{\text{tag}}$  and a semileptonic  $B \rightarrow D^{(*)} \ell \nu$  decay in data and MC. As the branching fractions for  $B \rightarrow D^{(*)} \ell \nu$  are precisely known, and their reconstruction efficiencies can be separately calculated, the difference between data and MC for  $B_{\text{tag}}$  reconstruction can be extracted. The resulting correction factor is  $0.64 \pm 0.03$ . The uncertainty in this value is taken as a systematic uncertainty.

The systematic uncertainty due to charged track reconstruction is evaluated using  $D^{*+} \rightarrow D^0 \pi^+$  decays, with  $D^0 \rightarrow K_S^0 \pi^+ \pi^-$  and  $K_S^0 \rightarrow \pi^+ \pi^-$ . The resulting uncertainty is 0.35% per track. The uncertainty due to lepton identification is evaluated using  $e^+ e^- \rightarrow e^+ e^- \gamma^* \gamma^* \rightarrow e^+ e^- \ell^+ \ell^-$  events. The resulting uncertainties are 1.6% for muons and 1.8% for electrons.

The systematic uncertainty in the signal reconstruction efficiency due to limited MC statistics is  $< 0.1\%$  for both signal modes. The systematic uncertainty arising from the number of  $B\bar{B}$  pairs is 1.4%, and the known uncertainty on  $f^{00}$  corresponds to a systematic uncertainty of 1.2%.

The total additive (in number of events) and multiplicative (in percent) systematic uncertainties are obtained by adding in quadrature all systematic uncertainties of that type.

## VII. SUMMARY

We have searched for the lepton-flavor-violating decays  $B^0 \rightarrow \tau^\pm \ell^\mp$  using the full Belle data set. We find no evidence for these decays and set the following upper limits on the branching fractions at 90% CL:

$$\mathcal{B}(B^0 \rightarrow \tau^\pm \mu^\mp) < 1.5 \times 10^{-5}, \quad (3)$$

$$\mathcal{B}(B^0 \rightarrow \tau^\pm e^\mp) < 1.6 \times 10^{-5}. \quad (4)$$

Our result for  $B^0 \rightarrow \tau^\pm \mu^\mp$  is very similar to a recent result from LHCb [15]. Our result for  $B^0 \rightarrow \tau^\pm e^\mp$  is the most stringent limit to date, improving upon the previous limit by almost a factor of two. We find no indication of lepton flavor violation in these decays.

## ACKNOWLEDGMENTS

We thank the KEKB group for the excellent operation of the accelerator; the KEK cryogenics group for the efficient operation of the solenoid; and the KEK computer group, and the Pacific Northwest National Laboratory (PNNL) Environmental Molecular Sciences Laboratory (EMSL) computing group for strong computing support; and the National Institute of Informatics, and Science Information NETwork 5 (SINET5) for valuable network support. We acknowledge support from the Ministry of Education, Culture, Sports, Science, and Technology (MEXT) of Japan, the Japan Society for the Promotion of Science (JSPS), and the Tau-Lepton Physics Research Center of Nagoya University; the Australian Research Council including Grants No. DP180102629, No. DP170102389, No. DP170102204, No. DP150103061, and No. FT130100303; Austrian Federal Ministry of Education, Science and Research (FWF) and FWF Austrian Science Fund No. P 31361-N36; the National Natural Science Foundation of China under Contracts No. 11435013, No. 11475187, No. 11521505, No. 11575017, No. 11675166, and No. 11705209; Key Research Program of Frontier Sciences, Chinese Academy of Sciences (CAS), Grant No. QYZDJ-SSW-SLH011; the CAS Center for Excellence in Particle Physics (CCEPP); the Shanghai Pujiang Program under Grant No. 18PJ1401000; the Shanghai Science and Technology Committee (STCSM) under Grant No. 19ZR1403000; the Ministry of Education, Youth and Sports of the Czech Republic under Contract No. LTT17020; Horizon 2020 ERC Advanced Grant No. 884719 and ERC Starting Grant No. 947006

“InterLeptons” (European Union); the Carl Zeiss Foundation, the Deutsche Forschungsgemeinschaft, the Excellence Cluster Universe, and the Volkswagen-Stiftung; Institut National de Physique Nuclaire et de Physique des Particules (IN2P3) du CNRS (France); the Department of Atomic Energy (Project Identification No. RTI 4002) and the Department of Science and Technology of India; the Istituto Nazionale di Fisica Nucleare of Italy; National Research Foundation (NRF) of Korea Grants No. 2016R1D1A1B01010135, No. 2016R1D1A1B02012900, No. 2018R1A2B3003643, No. 2018R1A6A1A06024970, No. 2018R1D1A1B07047294, No. 2019K1A3A7A09033840, and No. 2019R1I1A3A01058933; Radiation Science Research Institute, Foreign Large-size Research Facility Application Supporting project, the Global Science Experimental Data Hub Center of the Korea Institute of Science and Technology Information and KREONET/GLORIAD; the Polish Ministry of Science and Higher Education and the National Science Center; the Ministry of Science and Higher Education of the Russian Federation, Agreement No. 14.W03.31.0026, and the HSE University Basic Research Program, Moscow; University of Tabuk research Grants No. S-1440-0321, No. S-0256-1438, and No. S-0280-1439 (Saudi Arabia); the Slovenian Research Agency Grants No. J1-9124 and No. P1-0135; Ikerbasque, Basque Foundation for Science, Spain; the Swiss National Science Foundation; the Ministry of Education and the Ministry of Science and Technology of Taiwan; and the United States Department of Energy and the National Science Foundation.

- 
- [1] Throughout this paper, charge-conjugate modes are implicitly included unless noted otherwise.
- [2] Y. Amhis *et al.* (Heavy Flavor Averaging Group), *Eur. Phys. J. C* **81**, 226 (2021); and online update at <https://hflav.web.cern.ch/>.
- [3] R. Aaij *et al.* (LHCb Collaboration), *J. High Energy Phys.* **08** (2017) 055.
- [4] R. Aaij *et al.* (LHCb Collaboration), *Phys. Rev. Lett.* **122**, 191801 (2019).
- [5] R. Aaij *et al.* (LHCb Collaboration), [arXiv:2103.11769](https://arxiv.org/abs/2103.11769).
- [6] S. Wehle *et al.* (Belle Collaboration), *Phys. Rev. Lett.* **126**, 161801 (2021).
- [7] J. P. Lees *et al.* (BABAR Collaboration), *Phys. Rev. D* **86**, 032012 (2012).
- [8] S. L. Glashow, D. Guadagnoli, and K. Lane, *Phys. Rev. Lett.* **114**, 091801 (2015).
- [9] X.-G. He, G. Valencia, and Y. Wang, *Phys. Rev. D* **70**, 113011 (2004); S. Fukuda *et al.* (Super-Kamiokande Collaboration), *Phys. Rev. Lett.* **85**, 3999 (2000); Q. R. Ahmad *et al.* (SNO Collaboration), *Phys. Rev. Lett.* **89**, 011301 (2002); K. Eguchi *et al.* (KamLand Collaboration), *Phys. Rev. Lett.* **90**, 021802 (2003); M. H. Ahn *et al.*, *Phys. Rev. Lett.* **90**, 041801 (2003).
- [10] Specifically, a tiny neutrino mass in the eV range.
- [11] A. D. Smirnov, *Mod. Phys. Lett. A* **33**, 1850019 (2018).
- [12] A. Dedes, J. Ellis, and M. Raidal, *Phys. Lett. B* **549**, 159 (2002).
- [13] A. Bornheim *et al.* (CLEO Collaboration), *Phys. Rev. Lett.* **93**, 241802 (2004).
- [14] B. Aubert *et al.* (BABAR Collaboration), *Phys. Rev. D* **77**, 091104(R) (2008).
- [15] R. Aaij *et al.* (LHCb Collaboration), *Phys. Rev. Lett.* **123**, 211801 (2019).
- [16] S. Kurokawa and E. Kikutani, *Nucl. Instrum. Methods Phys. Res., Sect. A* **499**, 1 (2003), and other papers included



- in this volume; T. Abe *et al.*, *Prog. Theor. Exp. Phys.* **2013**, 03A001 (2013) and following articles up to 03A011.
- [17] Z. Natkaniec *et al.* (Belle SVD2 Group), *Nucl. Instrum. Methods Phys. Res., Sect. A* **560**, 1 (2006).
- [18] A. Abashian *et al.* (Belle Collaboration), *Nucl. Instrum. Methods Phys. Res., Sect. A* **479**, 117 (2002); also see detector section in J. Brodzicka *et al.*, *Prog. Theor. Exp. Phys.* **2012**, 04D001 (2012).
- [19] D. J. Lange, *Nucl. Instrum. Methods Phys. Res., Sect. A* **462**, 152 (2001).
- [20] T. Sjöstrand, S. Mrenna, and P. Skands, *J. High Energy Phys.* **05** (2006) 026.
- [21] E. Barberio, B. van Eijk, and Z. Was, *Comput. Phys. Commun.* **66**, 115 (1991).
- [22] R. Brun *et al.*, CERN Report No. DD/EE/84-1, 1984.
- [23] P. A. Zyla *et al.* (Particle Data Group), *Prog. Theor. Exp. Phys.* **2020**, 083C01 (2020).
- [24] M. Feindt, F. Keller, M. Kreps, T. Kuhr, S. Neubauer, D. Zander, and A. Zupanc, *Nucl. Instrum. Methods Phys. Res., Sect. A* **654**, 432 (2011).
- [25] E. Nakano, *Nucl. Instrum. Methods Phys. Res., Sect. A* **494**, 402 (2002).
- [26] A. Abashian *et al.*, *Nucl. Instrum. Methods Phys. Res., Sect. A* **491**, 69 (2002).
- [27] K. Hanagaki, H. Kakuno, H. Ikeda, T. Iijima, and T. Tsukamoto, *Nucl. Instrum. Methods Phys. Res., Sect. A* **485**, 490 (2002).
- [28] A. Sibidanov *et al.* (Belle Collaboration), *Phys. Rev. D* **88**, 032005 (2013).